Title

Exciton and phonon dynamics in highly aligned 7-atom wide armchair graphene nanoribbons as seen by time-resolved spontaneous Raman scattering

Journal

Nanoscale, 10(37)

ISSN

2040-3364

Authors

Zhu, Jingyi
German, Raphael
Senkovskiy, Boris V
et al.

Publication Date

2018-09-27

DOI

10.1039/c8nr05950k

Peer reviewed

Exciton and Phonon Dynamics in Highly Aligned 7-Armchair Graphene Nanoribbons as Seen by Time-resolved Spontaneous Raman Scattering

Jingyi Zhu,† Raphael German,† Boris Senkovskiy,† ..... Felix R. Fischer,‡ Alexander Grüneis,† and Paul H. M. van Loosdrecht*,†

† Physics institute 2, University of Cologne, 50937, Germany

‡ Department of Chemistry, University of California at Berkeley, Tan Hall 680, Berkeley, California 94720, United States

Supporting Information Placeholder

ABSTRACT: The opening of a band gap in graphene nanoribbons induces novel optical and electronic properties, strongly enhancing their application potential in nanoscale devices. Knowledge of the optical excitations and associated relaxation dynamics are essential for developing and optimizing device designs and functionality. Here we report on the optical excitations and associated relaxation dynamics in surface aligned 7-armchair graphene nanoribbons as seen by time-resolved spontaneous Stokes and anti-Stokes Raman scattering spectroscopy. On the anti-Stokes side we observe an optically induced increase of the scattering intensity of the Raman active optical phonons which we assign to changes in the optical phonon populations. The optical phonon population decays with a lifetime of ~2 ps, indicating an efficient optical-acoustic phonon cooling mechanism. On the Stokes side we observe a substantial decrease of the phonon peak intensities which we relate to the dynamics of the optically induced exciton population. The exciton population shows a multi-exponential relaxation on the hundreds of ps time scale, independent of the excitation intensity. Our results shed light on the optically induced phonon and exciton dynamics in surface aligned armchair graphene nanoribbons and demonstrate that time-resolved spontaneous Raman scattering spectroscopy is a powerful method for exploring quasi-particle dynamics in low dimensional materials.

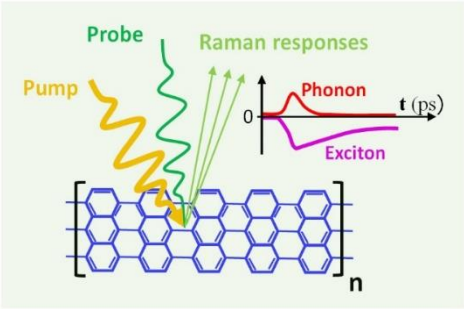

INTRODUCTION

Graphene based nanostructures have been attracting widespread attention in research and industry[1-5] since the first graphene electronic device was demonstrated in 2004.[6] Of particular interests are the spatially confined strips of graphene monolayer, dubbed graphene nanoribbons (GNRs). Due to one-dimensional quantum confinement and edge dependent effects, these GNRs display remarkable chemical, electrical and optical properties, including a width-tunable band gap, excitonic optical transition, and room temperature ballistic transport.[7-11] These novel properties result in many potential applications in nanoscale electronic transistor devices,[12,13] optical modulators,[14] quantum gates,[15] and infrared photodetectors.[16,17] The development of applications, as well as the fundamental understanding of the GNRs electronic properties requires knowledge of the fundamental optical excitation properties and energy relaxation mechanisms in these one dimensional systems.

Over the past, electronic structures and excitation properties of GNRs have been investigated via conventional spectroscopic techniques such as X-Ray absorption,[18,19] scanning tunneling,[20,21] and photoelectron spectroscopy[22-24]. In addition the electronic structure has been studied from a theoretical point of view.[25-28] The general steady state features such as the band gap structure of GNRs are reasonably well understood by now. Studies on the dynamical non-equilibrium properties of GNRs are, however, more scarce most likely due to lack of sufficiently sensitive experimental techniques for these single layered materials. Recently, polarized reflectance measurements combined with ab initio calculations[11,29] demonstrated

that the optical absorption in armchair graphene nanoribbons (AGNRs) are dominated by excitonic transitions. The investigation of the electronic relaxation dynamics in graphene based nanomaterials has been limited to a few cases reporting transient absorption spectroscopy measurements of solution solvated and suspended samples,[30-32] and time resolved terahertz studies of multilayer aggregated GNRs.[33,34] The development of methods to grow aligned GNRs on gold surfaces,[35] and techniques to transfer the GNRs to non-metallic substrates[36] opened the possibility to study the properties of GNRs in a more controlled manner, including for instance symmetry aspects using polarization sensitive spectroscopies.

Steady state Raman spectroscopy has been proven to be a versatile tool in the characterization of carbon and graphene based materials.[37-39] It allows to determine the number and orientation of layered graphene, yields information on strain, doping, and disorder, and provides a good method to assess the quality of graphene based materials as well as the nature of edges and functional groups in functionalized graphene.[40,41] In addition to this, the time-resolved variant of Raman spectroscopy is a powerful method to investigate both incoherent phonon relaxation as well as electron-phonon coupling and electronic dynamics.[42-49]

In this report, we applied these spectroscopic techniques to study the optical transition properties and in particular the optically induced phonon and electronic dynamics in 7-AGNRs aligned on a silica/silicon substrate. We demonstrated that not only the phonon population, but also the excitonic relaxation dynamics, can be extracted from the optically induced changes in the Raman spectrum. To achieve the latter, we make use of the strong resonant enhancement of the optical phonon Raman scattering due to excitonic transitions. The observed fast phonon creation and relaxation originates from an efficient exciton-phonon and optical-acoustical phonon coupling, respectively, indicating of an efficient energy dissipation in this material. The observed strong resonant optical transition and non-exponential nature of the excitonic relaxation in this one dimensional system evidences the dominated existence of dark and trapped exciton states. These knowledge provide fundamental understanding of the GNRs system toward further optimizing electronic device application.

METHODS

Sample preparation. 7-AGNRs were synthesized using the well-established bottom-up fabrication approach on Au (788) surfaces which exhibit a regular arrays of narrow (111) terraces dictating the direction of growth and yielding high quality, densely aligned ribbons.[22,35] The transfer from the Au (788) substrate to the insulating silica/silicon substrate was performed by the alignment-preserving bubbling transfer method based on an electrochemical delamination process.[50,51]

Experimental Setup. Steady state (one laser beam) Raman spectra of 7-AGNRs were performed using a micro-Raman setup equipped with a tandem triple spectrometer (Spectroscopy & Imaging GmbH) and LN2 cooled CCD (PyLoN 100; Princeton Instruments). An optical parametric amplifier (OPA, Light conversion), pumped by a single-unit amplified femtosecond laser (Pharos, Light conversion) running at a repetition rate of 100 kHz provided wavelength tunable (400 nm to 800 nm; 1.5-3.1 eV) picosecond pulses (~2 ps) as excitation source. The excitation pulses were spectrally cleaned and narrowed (full width a half maximum (FWHM) ~10 cm^{-1}) using a home build pulse shaper. The pulses were focused on the sample with a 20 times micro objective, and Raman signals were collected in a backscattering geometry. To avoid sample degradation, samples were mounted in a cryostat pumped down to 10^{-5} mbar.

Time-resolved measurements (Figure 1a) of 7-AGNRs were performed with the same setup by introducing a pump laser pulse (~300 fs) provided by a second OPA (ORPHEUS, Light conversion) pumped by the same amplified laser. The samples were pumped with laser wavelengths of 590 nm (2.1 eV) and 490 nm (2.5 eV) respectively, and Raman signal were collected using 512 nm (2.4 eV) probe pulses (Figure 1c). Both the pump and probe light polarization are parallel to the long axis of the AGNRs. In order to avoid optical damage of the samples and improve the signal to noise ratio, the laser spot sizes on the sample were defocused to ~60 μm. The back reflected Raman scattering signals were re-collimated with an additional telescope lens group before entering the spectrometer.

RESULTS

Figure 1b presents typical steady state polarized Raman scattering spectra of the 7-AGNRs on Stokes side. The phonon scattering peak at around 521 cm^{-1} originates from the silica/silicon substrate and provides a good reference for the measurements. The highly orientated nature of our samples is demonstrated by the strong enhancement (~ 10x) of the Raman signal when the incoming light is polarized along the ribbons.[36] The G and D modes typical for all graphene related materials are clearly observed in the spectra. The C-C stretching G mode, located at 1608 cm^{-1}, corresponds to a carbon-carbon bond stretching mode along the ribbon. The D mode which can be related to defects or the edges of GNRs[52] is found at 1345 cm^{-1} and is weaker than the G mode. Other vibrational Raman peaks,[53] like the radial breathing mode related to the ribbon width expansion is found at 398 cm^{-1}, and the confinement-derived vibrational modes at 1255 cm^{-1} and 1266 cm^{-1} were also well resolved. In general, the spectra measured with the pulsed laser are fully consistent with previous results measured on 7-AGNRs on a metallic substrate surface[36,54] with continuum laser beams.

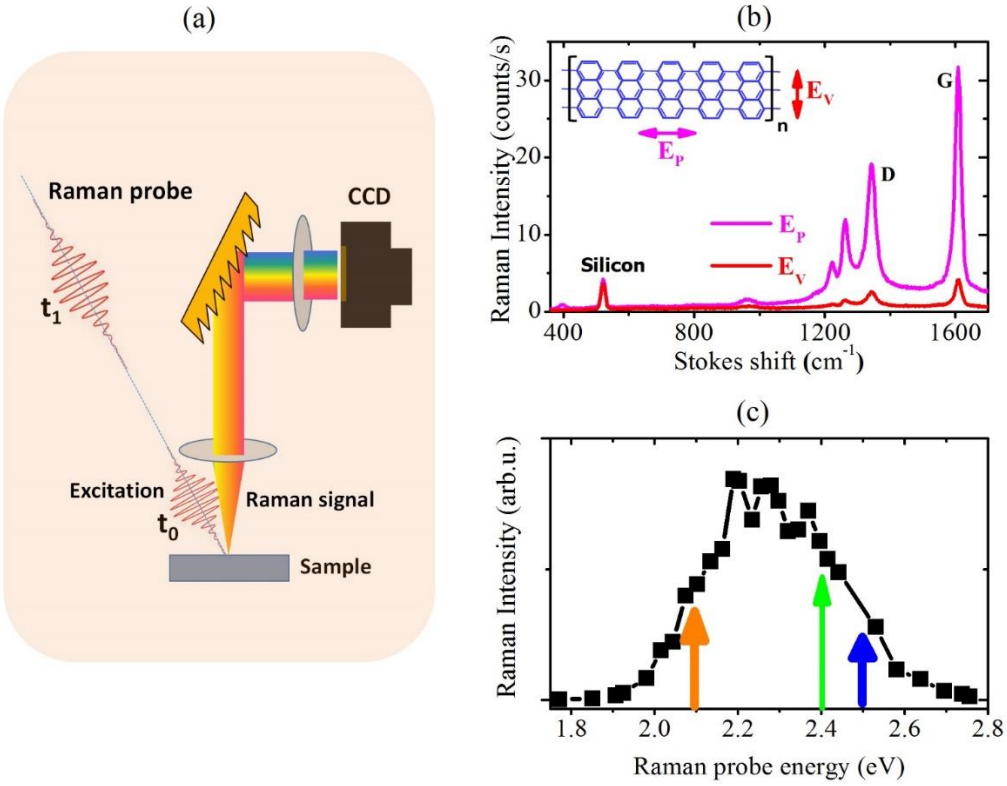

Figure 1. (a) Illustration of steady state and time-resolved spontaneous Raman scattering experiments. Steady state measurement is obtained when the pump beam is blocked. (b) Steady state Raman scattering spectra of the 7-AGNRs on silica/silicon recorded with picosecond pulsed laser at 512 nm, E_P indicates that the polarization of laser pulse is along the ribbons, E_V indicates that the polarization of laser pulse perpendicular to the ribbons. (c) Energy dependence of the Raman intensity of the phonon G peak, showing a strong resonant enhancement of the Raman scattering. Dark yellow and blue arrows indicate the pump energies used for the time-resolved experiments, green arrow indicate the Raman probe energy used for the data shown in (a) and for the time-resolved experiments.

To investigate resonance effects due to optical transitions in 7-AGNRs, wavelength dependent Raman scattering measurements were performed. Figure 1c depicts the resonance profile of the integrated intensity of the G mode (for the spectra see Figure S1). A clear resonant profile was observed, centered at ~ 2.3 eV with a FWHM of ~0.4 eV. The observed resonant profile resembles the imaginary part of the dielectric function of 7-AGNRs on a gold substrate, which was interpreted in terms of an excitonic transition.[11] The fundamental energy gap for 7-AGNRs on a gold surface is strongly reduced due to polarization screening by the substrate compared to the theoretically calculated energy gap of ~ 3.7 eV.[11] In our case one expects a much weaker screening by the silica/silicon substrate, and hence a substantially higher single particle band gap. Indeed, it has been demonstrated that the reduced screening for 7-AGNRs aligned on an Au-Silicon alloy substrate leads to a band gap of 2.7 eV.[55] Since the dielectric constant of our silica/silicon substrate is even lower, we expect a single particle band gap much closer to the theoretical value of 3.7 eV. In view of this we can safely assign the observed resonance around 2.3 eV in the Raman scattering experiment to excitonic transitions associated with an exciton binding energy of the order of 1 eV.

Figure 2a depicts the time-resolved Stokes spectra after optical excitation at 590 nm (2.1 eV), with excitation laser intensity around 1.2×10^{14} photons/cm^2. To more clearly exhibit the pump induced effects on the Raman spectra, Figure 2b shows difference spectra obtained by subtracting the -5 ps spectrum (top panel Figure 2a) from the time delayed spectra in Figure 2a. As is clear from the figures, the Raman spectra show an overall decrease of scattering intensity for all time delays, which recovers on a hundreds of ps time scale. Similar spectral changes were also observed upon excitation at higher photon energy at 490 nm (2.5 eV) (Figure S2). These observations contrast the usual observations in time resolved spontaneous Raman experiments of an increasing optical phonon scattering intensity originates from an, through the electron-phonon scattering processes, optically increased phonon population.[45,48,56] This surprising result can be understood in terms of optically induced changes in the Raman resonance efficiency which allows extraction of the electronic relaxation dynamics from our data, as we will discuss later on in this report.

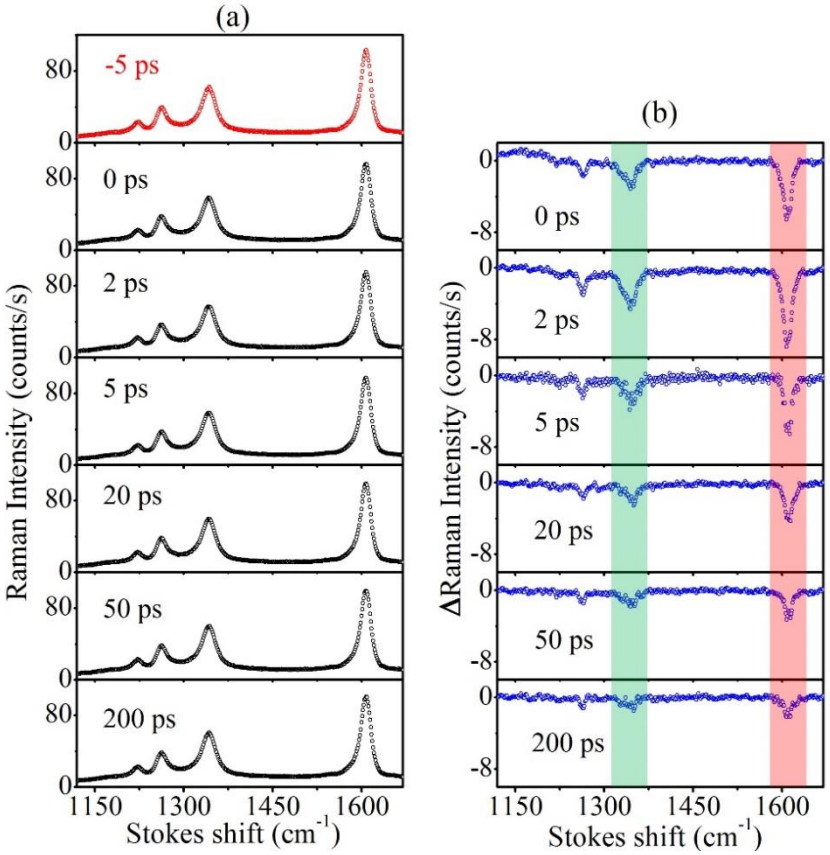

Figure 2. Time-resolved spontaneous Raman scattering spectra of the 7-AGNRs recorded on Stokes side, with pump energy at 2.1 eV and Raman probe energy at 2.4 eV. (a) Raman scattering intensity spectra at different delay times after optical excitation. (b) Difference spectra obtained by subtraction the spectrum at -5 ps from each spectrum in (a) at different corresponding delay time. The color bars indicate the integration regions used in the analysis of the transient behavior.

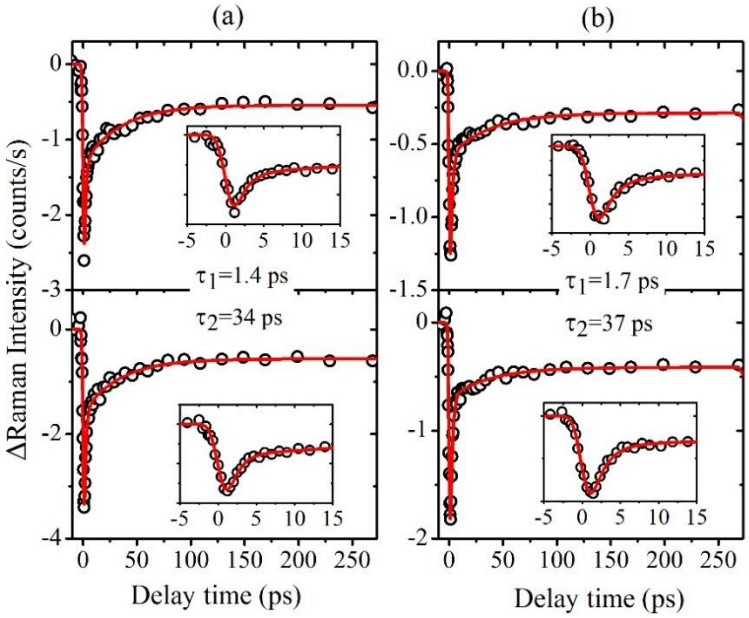

Figure 3. Decay dynamics of the phonon peak D (top panels) and G (bottom panels). (a) Dynamics observed at the excitation wavelength of 590 nm (2.1 eV). (b) Dynamics observed at the excitation wavelength of 490 nm (2.5 eV). Black circles represent the experimental data, red lines represent a global fitted. Insets show the short time dynamics.

To obtain a more detailed insight into the dynamics, the changes in the phonon scattering intensities of the D and G bands are integrated (over regions indicated by the colored areas in Figure 2b) for each time delay. The dynamics of the D and G bands are plotted in Figure 3 and are found to be identical: the changes in the Stokes spectra show a substantial decay within 100s of ps, but only fully recover on a ns time scale, which is out of our detection window. Multi-exponential decay functions are required to fit the data, where a global fitting of the D and G responses yield decay times of 1.4 ps and 34 ps for the 2.1 eV pumped spectra, and 1.7 and 37 ps for the 2.5 eV pumped spectra. The 20-40 ps decay dynamics observed is much longer than the general optical phonon population dynamics in graphite and graphene related systems[44,45,48,49,56] which are in the time range of 1-2 ps. On the other hand, the time behaviors are comparable to the exciton recombination dynamics as observed in graphene nanotubes[31,57] and nanoribbons.[30] This, together with the resonant nature of the Raman scattering, strongly suggests that an exciton related relaxation mechanism is responsible for the observations.

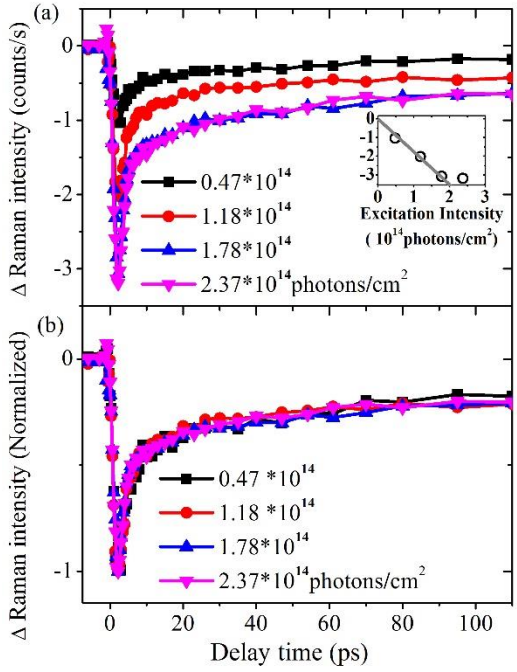

Figure 4. Pump (2.1 eV) excitation intensity dependence of the decay dynamics. The data represent the averaged response of the D and G bands. In (a) the raw data are presented and in (b) data are normalized to show the absence of the pump intensity dependent dynamics. The inset in (a) shows the pump excitation intensity dependence of the amplitude at a delay of 2 ps.

To test if any many-body relaxation mechanisms are involved in the decay of the Stokes response, excitation intensity dependent measurements are carried out with the pump photon energy at 2.1 eV. The measured results are presented in Figure 4. Since dynamics form D and G peaks are generally the same, only the average of the D and G responses is plotted. For pump excitation densities < 2×10^{14} photons/cm^2 a linear increase of the signal is observed which seem to saturate above this value (see inset in Figure 4a). Figure 4b, which shows the same data normalized to the maximum response, indicates that there is no pump excitation power dependence in the dynamics, demonstrating the absence of many-body processes in the transient behavior of the signal.

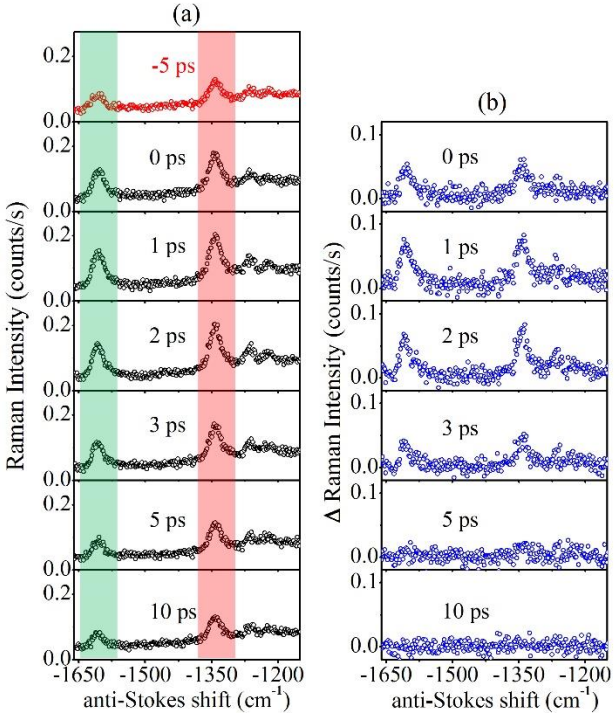

Figure 5. Time-resolved spontaneous Raman scattering spectra of the 7-AGNRs recorded on anti-Stokes side. (a) Raman scattering intensity spectra at different delay times after optical excitation at 2.1 eV. (b) Pump induced difference spectra obtained by subtraction the spectrum at -5 ps from each spectrum in (a) at different corresponding delay times.

It is clear from the above that the dynamics of the phonon population cannot be extracted from the Stokes side Raman spectra. In order to obtain insight in the phonon population dynamics we have therefore carried out time-resolved experiments on anti-Stokes side, using identical experimental conditions with a pump energy of 2.1 eV and pump intensity of 1.2×10^{14} photons/cm^2. The recorded time dependent spectra are presented in Figure 5, in the same manner as those on Stokes side in Figure 2. Indeed a pump induced enhancement of the phonon scattering signals is observed for both D and G responses on the anti-Stokes side. The dynamics show a very fast response, with ingrowth times faster than our time resolution and decay time of ~2 ps. The integrated intensity dynamics for the D and G responses are shown in Figure 6a, both have identical relaxation dynamics. A global single exponential

fit yields a decay constant of 1.9 ps, which can be interpreted as the lifetime of the optical phonons.

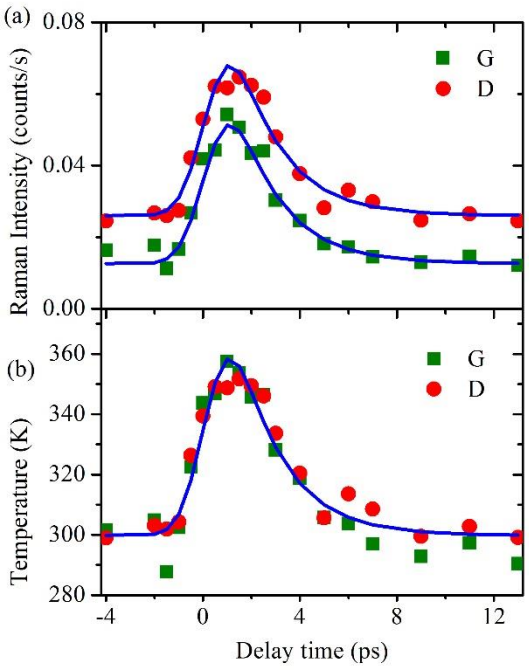

Figure 6. Phonon population dynamics of 7-AGNRs extracted from anti-Stokes spectra. (a) Dynamics obtained for peak D and G (symbols are experimental data; lines represent a global single exponential fit convoluted with the instrumental response.). (b) Calculated transient phonon temperatures for the D and G responses.

In principle, phonon temperatures[58,59] can be obtained from the signal ratio between Stokes and anti-Stokes side, based on the detailed balance resulted from fluctuation-dissipation theorem. However, due to the strong resonance Raman effects this is not trivial. We therefore estimated the transient optical phonon temperature using the reasonable assumption (Supporting Information) that before time zero the phonon temperatures are equal to the environment temperature (~300 K). As indicated in Figure 6b, the transient temperatures estimated from both D and G peaks are, within the experimental accuracy, identical and reach a maximum value of 350 K within our time resolution. They decay to the equilibrium temperature within 2 ps as the optical phonons are depopulated through optical-acoustical phonon scattering.

DISCUSSION

The decay dynamics of the optical phonons in 7-AGNRs is found to be very similar to the dynamics observed in in graphite and graphene nanotubes.[48,56] The main difference is in the observed temperature increase which is only 50 K in 7-AGNRs and can exceed 1000 K in graphite under similar excitation conditions[48]. Correspondingly, the phonons in 7-AGNRs also do not show any spectral dynamics such as the stiffening observed in graphite. These differences originate from the generation mechanism of the optical phonons. In the experiments on graphite the optically induced phonon population is created through relaxation of the highly excited free carriers to the conduction band minimum. In our experiments on the 7-AGNRs, however, the optical transitions are excitonic in nature and excited with only a limited amount of excess energy (*i.e.* close to resonant excitation), leading to a much lower raise of the phonon population, and thus phonon temperature, as compared to the graphite case.

The most interesting observation reported here is arguably the decay dynamics of the Stokes spectra. Since we are directly exciting the excitonic transition responsible for the resonant Raman enhancement, the transient decay of the Stokes response directly reflects the exciton dynamics of the 7-AGNRs (see Supporting Information). The reduction of the resonant enhancement is a direct consequence of ground state bleaching/excited state filling, *i.e.* of the reduction of the optical transition probability. We note that pump-probe Terahertz conductivity experiments on multi-layered AGNRs[34] showed a short lived dynamics (1-2ps) which has been assigned to free carrier relaxation caused by the formation of excitons. Though we observe a similar fast time scale of the initial decay of the Stokes response, its origin has a different nature. Our steady state resonant Raman results demonstrate the pure excitonic nature of the transitions around 2.3 eV in 7-AGNRs, therefore one does not expect any substantial density of free carriers directly after pump excitation. This is corroborated by the observation that the dynamics and amplitudes of the signal are nearly identical for both excitation energies used in the experiments (2.1 eV and 2.5 eV, see Figure 3), and by the observation that the fast decay components recovers around 50% of the initial amplitude. The latter would not be expected if formation of excitons from free carriers is responsible for the initial fast decay since such a process does not substantially recover the optically induced ground state bleaching and thus the changes in the Raman resonance enhancement.

Since 7-AGNRs are non-luminescent,[36] exciton recombination must be non-radiative decay process. In carbon nanotubes, non-radiative exciton relaxation decay proceeds by passing through either long-lived defect related trap states ,[60] or through scattering into the optically inactive dark exciton states.[61] Also in the AGNRs one expects both trap and dark states. The dark states are derived from the E12 (upper valence band to second conduction band) and E21 (second valence band to lowest conduction band) transitions, whereas defect related trap states (both short and long lived) are expected to be present either originating from the bottom up growth process or from the electrochemical transfer process. The observed decay dynamics can now be understood as follows. After the initial creation of the free exciton population excitons populate both dark as well as trap states. Within the first

2 ps part of this population (short lived trap states) recombine, thereby reducing the transient response. In the following 30 ps dark excitons decay non-radiatively, leaving only the long lived trap exciton states, which amount to about 20% of the initial excited exciton population. These latter then decay on a nanosecond timescale which is out of our observation window.

In most graphene based nanomaterials, such as the carbon nanotubes[57,62,63] and a cove-shaped graphene nanoribbons,[30] diffusion controlled exciton-exciton annihilation dominates the exciton relaxation processes. Our experiments have shown that in our case many-body processes do not play a dominant role. This is understandable in view of the relatively short length[22] of the 7-AGNRs (~50 nm) compared to carbon nanotubes (exceeding 1 μm) and the mild excitation conditions used in our experiments: one does not expect a substantial amount of AGNRs with more than one exciton excited and hence no exciton-exciton annihilation processes.

SUMMARY

In summary, wavelength dependent Raman scattering confirmed the excitonic nature of the 2.3 eV optical band gap in 7-AGNRs on a silica/silicon substrate. The estimated exciton binding energy is about 1 eV. Optical excitation of these excitons leads to an enhanced optical phonon population through relaxation of the excess exciton energy by exciton-phonon scattering on a time scale faster than our temporal resolution (~1.5 ps). The decay times of the optical D and G phonon populations, originating from optical-acoustic phonon scattering, are found to be ~2 ps, similar to values found in other graphene based nanomaterials and graphite. The exciton dynamics is directly reflected in the optical induced changes of Raman susceptibility. No evidence for diffusion controlled exciton-exciton recombination has been found, consistent with expectations. The exciton relaxation is found to be multi-exponential (decay constants ~1.5 , ~30 ps and >1 ns) reflecting the presence of short and long lived trap states as well as the expected dark states which have a life time of ~30 ps.

ASSOCIATED CONTENT

Supporting Information

Phonon temperature estimation methods, Raman tensor reduction vs exaction population model description and supporting figures are included in the Supporting Information. "This material is available free of charge via the Internet at http://pubs.acs.org."

AUTHOR INFORMATION

Corresponding Author

*pvl@ph2.uni-koeln.de.

ACKNOWLEDGMENT

Financial support by the Deutsche Forschungsgemeinschaft (DFG) through CRC1238 (projects B05 and A01) and project INST 216/798-1 is gratefully acknowledged. A.G. and B.S. acknowledge the ERC grant no. 648589 ' SUPER-2D '.

TOC

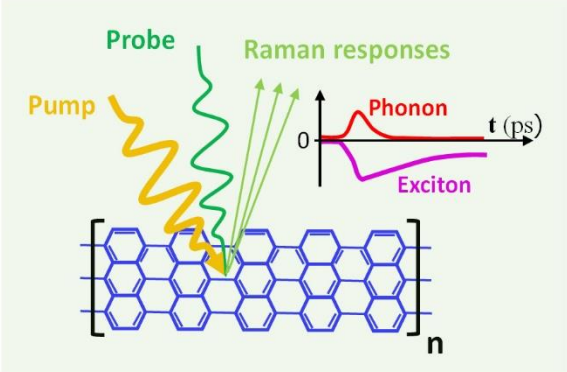

REFERENCES

(1) Narita, A.; Wang, X. Y.; Feng, X. L.; Mullen, K. *Chem Soc Rev* **2015**, *44*, 6616.

(2) Allen, M. J.; Tung, V. C.; Kaner, R. B. *Chem Rev* **2010**, *110*, 132.

(3) Bonaccorso, F.; Sun, Z.; Hasan, T.; Ferrari, A. C. *Nat Photonics* **2010**, *4*, 611.

(4) Avouris, P.; Freitag, M. *Ieee J Sel Top Quant* **2014**, *20*.

(5) Enyashin, A. N.; Ivanovskii, A. L. *Phys Status Solidi B* **2011**, *248*, 1879.

(6) Novoselov, K. S.; Geim, A. K.; Morozov, S. V.; Jiang, D.; Zhang, Y.; Dubonos, S. V.; Grigorieva, I. V.; Firsov, A. A. *Science* **2004**, *306*, 666.

(7) Wakabayashi, K.; Sasaki, K.; Nakanishi, T.; Enoki, T. *Sci Technol Adv Mat* **2010**, *11*.

(8) Alfonsi, J.; Meneghetti, M. *New J Phys* **2012**, *14*.

(9) Baringhaus, J.; Ruan, M.; Edler, F.; Tejeda, A.; Sicot, M.; Taleb-Ibrahimi, A.; Li, A. P.; Jiang, Z. G.; Conrad, E. H.; Berger, C.; Tegenkamp, C.; de Heer, W. A. *Nature* **2014**, *506*, 349.

(10) Palacios, J. J. *Nat Phys* **2014**, *10*, 182.

(11) Denk, R.; Hohage, M.; Zeppenfeld, P.; Cai, J.; Pignedoli, C. A.; Sode, H.; Fasel, R.; Feng, X.; Mullen, K.; Wang, S.; Prezzi, D.; Ferretti, A.; Ruini, A.; Molinari, E.; Ruffieux, P. *Nat Commun* **2014**, *5*, 4253.

(12) Schwierz, F. *Nat Nanotechnol* **2010**, *5*, 487.

(13) Lemme, M. C.; Echtermeyer, T. J.; Baus, M.; Kurz, H. *Ieee Electr Device L* **2007**, *28*, 282.

(14) Zhang, H.; Miyamoto, Y.; Cheng, X. L.; Rubio, A. *Nanoscale* **2015**, *7*, 19012.

(15) Karafyllidis, I. G. *J Comput Sci-Neth* **2015**, *11*, 326.

(16) Ahmadi, E.; Asgari, A.; Ahmadiniar, K. *Superlattice Microst* **2012**, *52*, 605.

(17) Ahmadi, E.; Asgari, A. *Phys Scripta* **2013**, *T157*.

(18) Zhu, X. H.; Hitchcock, A. P.; Bittencourt, C.; Umek, P.; Kruger, P. *J Phys Chem C* **2015**, *119*, 24192.

(19) Guttmann, P.; Bittencourt, C.; Rehbein, S.; Umek, P.; Ke, X. X.; Van Tendeloo, G.; Ewels, C. P.; Schneider, G. *Nat Photonics* **2012**, *6*, 25.

(20) Sode, H.; Talirz, L.; Groning, O.; Pignedoli, C. A.; Berger, R.; Feng, X. L.; Mullen, K.; Fasel, R.; Ruffieux, P. *Phys Rev B* **2015**, *91*.

(21) Kimouche, A.; Ervasti, M. M.; Drost, R.; Halonen, S.; Harju, A.; Joensuu, P. M.; Sainio, J.; Liljeroth, P. *Nat Commun* **2015**, *6*.

(22) Linden, S.; Zhong, D.; Timmer, A.; Aghdassi, N.; Franke, J. H.; Zhang, H.; Feng, X.; Mullen, K.; Fuchs, H.; Chi, L.; Zacharias, H. *Phys Rev Lett* **2012**, *108*.

(23) Ruffieux, P.; Cai, J. M.; Plumb, N. C.; Patthey, L.; Prezzi, D.; Ferretti, A.; Molinari, E.; Feng, X. L.; Mullen, K.; Pignedoli, C. A.; Fasel, R. *Acs Nano* **2012**, *6*, 6930.

(24) Della Pia, A.; Avvisati, G.; Ourdjini, O.; Cardoso, C.; Varsano, D.; Prezzi, D.; Ferretti, A.; Mariani, C.; Betti, M. G. *J Phys Chem C* **2016**, *120*, 7323.

(25) Yang, L.; Cohen, M. L.; Louie, S. G. *Nano Lett* **2007**, *7*, 3112.

(26) Prezzi, D.; Varsano, D.; Ruini, A.; Marini, A.; Molinari, E. *Phys Rev B* **2008**, *77*.

(27) Zhu, X.; Su, H. B. *J Phys Chem C* **2010**, *114*, 17257.

(28) Zhu, X.; Su, H. B. *J Phys Chem A* **2011**, *115*, 11998.

(29) Denk, R.; Lodi-Rizzini, A.; Wang, S.; Hohage, M.; Zeppenfeld, P.; Cai, J.; Fasel, R.; Ruffieux, P.; Berger, R. F. J.; Chen, Z.; Narita, A.; Feng, X.; Mullen, K.; Biagi, R.; De Renzi, V.; Prezzi, D.; Ruini, A.; Ferretti, A. *Nanoscale* **2017**, *9*, 18326.

(30) Soavi, G.; Dal Conte, S.; Manzoni, C.; Viola, D.; Narita, A.; Hu, Y. B.; Feng, X. L.; Hohenester, U.; Molinari, E.; Prezzi, D.; Mullen, K.; Cerullo, G. *Nat Commun* **2016**, *7*.

(31) Zhu, Z. P.; Crochet, J.; Arnold, M. S.; Hersam, M. C.; Ulbricht, H.; Resasco, D.; Hertel, T. *J Phys Chem C* **2007**, *111*, 3831.

(32) Chmeliov, J.; Narkeliunas, J.; Graham, M. W.; Fleming, G. R.; Valkunas, L. *Nanoscale* **2016**, *8*, 1618.

(33) Jensen, S. A.; Ulbricht, R.; Narita, A.; Feng, X. L.; Mullen, K.; Hertel, T.; Turchinovich, D.; Bonn, M. *Nano Lett* **2013**, *13*, 5925.

(34) Chen, Z. P.; Wang, H. I.; Teyssandier, J.; Mali, K. S.; Dumslaff, T.; Ivanov, I.; Zhang, W.; Ruffieux, P.; Fasel, R.; Rader, H. J.; Turchinovich, D.; De Feyter, S.; Feng, X. L.; Klaui, M.; Narita, A.; Bonn, M.; Mullen, K. *J Am Chem Soc* **2017**, *139*, 3635.

(35) Cai, J. M.; Ruffieux, P.; Jaafar, R.; Bieri, M.; Braun, T.; Blankenburg, S.; Muoth, M.; Seitsonen, A. P.; Saleh, M.; Feng, X. L.; Mullen, K.; Fasel, R. *Nature* **2010**, *466*, 470.

(36) Senkovskiy, B. V.; Pfeiffer, M.; Alavi, S. K.; Bliesener, A.; Zhu, J.; Michel, S.; Fedorov, A. V.; German, R.; Hertel, D.; Haberer, D.; Petaccia, L.; Fischer, F. R.; Meerholz, K.; van

Loosdrecht, P. H.; Lindfors, K.; Gruneis, A. *Nano Lett* **2017**.

(37) Ferrari, A. C.; Robertson, J. *Philos T Roy Soc A* **2004**, *362*, 2269.

(38) Ferrari, A. C. *Solid State Commun* **2007**, *143*, 47.

(39) Ferrari, A. C.; Robertson, J. *Philos T R Soc A* **2004**, *362*, 2477.

(40) Ferrari, A. C.; Basko, D. M. *Nat Nanotechnol* **2013**, *8*, 235.

(41) Neumann, C.; Reichardt, S.; Venezuela, P.; Drogeler, M.; Banszerus, L.; Schmitz, M.; Watanabe, K.; Taniguchi, T.; Mauri, F.; Beschoten, B.; Rotkin, S. V.; Stampfer, C. *Nat Commun* **2015**, *6*.

(42) Kash, J. A.; Tsang, J. C.; Hvam, J. M. *Phys Rev Lett* **1985**, *54*, 2151.

(43) Tsen, K. T.; Morkoc, H. *Phys Rev B* **1988**, *38*, 5615.

(44) Kang, K.; Ozel, T.; Cahill, D. G.; Shim, M. *Nano Lett* **2008**, *8*, 4642.

(45) Song, D. H.; Wang, F.; Dukovic, G.; Zheng, M.; Semke, E. D.; Brus, L. E.; Heinz, T. F. *Phys Rev Lett* **2008**, *100*.

(46) Fausti, D.; Misochko, O. V.; van Loosdrecht, P. H. M. *Phys Rev B* **2009**, *80*.

(47) Saichu, R. P.; Mahns, I.; Goos, A.; Binder, S.; May, P.; Singer, S. G.; Schulz, B.; Rusydi, A.; Unterhinninghofen, J.; Manske, D.; Guptasarma, P.; Williamsen, M. S.; Rubhausen, M. *Phys Rev Lett* **2009**, *102*, 177004.

(48) Yan, H. G.; Song, D. H.; Mak, K. F.; Chatzakis, I.; Maultzsch, J.; Heinz, T. F. *Phys Rev B* **2009**, *80*.

(49) Nesbitt, J. M.; Smith, D. C. *Nano Lett* **2013**, *13*, 416.

(50) Gao, L. B.; Ren, W. C.; Xu, H. L.; Jin, L.; Wang, Z. X.; Ma, T.; Ma, L. P.; Zhang, Z. Y.; Fu, Q.; Peng, L. M.; Bao, X. H.; Cheng, H. M. *Nat Commun* **2012**, *3*.

(51) Wang, Y.; Zheng, Y.; Xu, X. F.; Dubuisson, E.; Bao, Q. L.; Lu, J.; Loh, K. P. *Acs Nano* **2011**, *5*, 9927.

(52) Sasaki, K.; Kato, K.; Tokura, Y.; Suzuki, S.; Sogawa, T. *Phys Rev B* **2012**, *85*.

(53) Gillen, R.; Mohr, M.; Maultzsch, J. *Phys Status Solidi B* **2010**, *247*, 2941.

(54) Huang, H.; Wei, D. C.; Sun, J. T.; Wong, S. L.; Feng, Y. P.; Castro Neto, A. H.; Wee, A. T. S. *Sci Rep-Uk* **2012**, *2*.

(55) Deniz, O.; Sanchez-Sanchez, C.; Dumslaff, T.; Feng, X. L.; Narita, A.; Mullen, K.; Kharche, N.; Meunier, V.; Fasel, R.; Ruffieux, P. *Nano Lett* **2017**, *17*, 2197.

(56) Kang, K.; Abdula, D.; Cahill, D. G.; Shim, M. *Phys Rev B* **2010**, *81*.

(57) Soavi, G.; Scotognella, F.; Viola, D.; Hefner, T.; Hertel, T.; Cerullo, G.; Lanzani, G. *Sci Rep-Uk* **2015**, *5*.

(58) Maher, R. C.; Hou, J.; Cohen, L. F.; Le Ru, E. C.; Hadfield, J. M.; Harvey, J. E.; Etchegoin, P. G.; Liu, F. M.; Green, M.; Brown, R. J.; Milton, M. J. *J Chem Phys* **2005**, *123*, 084702.

(59) Maher, R. C.; Cohen, L. F. *J Phys Chem A* **2008**, *112*, 1497.

(60) Wang, F.; Dukovic, G.; Brus, L. E.; Heinz, T. F. *Phys Rev Lett* **2004**, *92*.

(61) Zhao, H. B.; Mazumdar, S. *Phys Rev Lett* **2004**, *93*.

(62) Russo, R. M.; Mele, E. J.; Kane, C. L.; Rubtsov, I. V.; Therien, M. J.; Luzzi, D. E. *Phys Rev B* **2006**, *74*.

(63) Allam, J.; Sajjad, M. T.; Sutton, R.; Litvinenko, K.; Wang, Z.; Siddique, S.; Yang, Q. H.; Loh, W. H.; Brown, T. *Phys Rev Lett* **2013**, *111*.